Int. J. Heat Mass Transfer. Vol. 14, pp. 825–834. Pergamon Press 1971. Printed in Great Britain

ANALYSIS OF FULLY-DEVELOPED ICE FORMATION IN A CONVECTIVELY-COOLED CIRCULAR TUBE

G. S. H. LOCK and R. H. NYREN
Department of Mechanical Engineering, University of Alberta, Edmonton, Alberta, Canada

(*Received* 24 *June* 1970 *and in revised form* 25 *September* 1970)

Abstract—The paper presents a theoretical analysis of ice formation in a long circular tube cooled by external convection. The analysis utilizes a regular perturbation expansion for the temperature and interface location: first order solutions are developed in closed form. The effects of ice sensible heat and external convection on the interface shape and the pressure gradient are shown graphically.

NOMENCLATURE

T, ϕ, temperature;
U, u, axial fluid velocity;
P, p, pressure;
R, r, radial displacement;
A, a, radial displacement of interface;
Θ, θ, angular displacement;
X, x, axial displacement;
t, τ, time;
S, area;
k, thermal conductivity;
ρ, density;
μ, kinematic viscosity;
L, latent heat;
C_p, specific heat;
κ, thermal diffusivity $[k/\rho\, C_p)]$;
h, heat-transfer coefficient in coolant;
Ste, Stefan number $[C_p(T_f - T_c)/L]$;
Bi, Biot number $[hR_1/k]$:
α, $Ste_i Bi_i/(1 + Bi_i)$.

Subscripts
$*$, fictitious surface;
1, tube surface inside;
0, tube centreline;
c, external coolant;
f, ice–water interface;
w, water;
i, ice;
ni, ice-free.

Superscript
$\hat{}$ circumferential average.

INTRODUCTION

One of the earliest attempts to analyze freezing in a cylindrical space was made in 1939 by Pekeris and Slichter [1] who considered ice formation on the outside of a long pipe the temperature of which varied in some prescribed manner beneath the freezing temperature. Their work, following the spirit of the classic paper by Stefan [2], employed a series expansion in which the zeroth order solution corresponded to the complete neglect of sensible heat in the ice: higher order terms incorporated the sensible heat, which was assumed to be a small fraction of the latent heat. Since that time several alternative approaches have appeared. London and Seban [3] used the concept of thermal circuitry to develop simple approximate solutions for both first and third kind boundary conditions. Kreith and Romie [4] presented analytic solutions for the situation in which the interface velocity remained constant and made use of an electric analogue to study the case of convective cooling. More recently, similar problems have been examined numerically [5, 6], using integral methods [7, 8] and by means of an analogue computer [9].

When ice begins to form in a convectively-cooled pipe the internal flow of water and the rate of ice formation are, in general, interrelated: the presence of ice alters the flow rate which then alters the heat flux leaving the water, and this in turn changes the rate of ice formation. In recent years, several authors [10–13] have studied this interrelation and demonstrated its significance in the developing, or thermal-entry, region corresponding to which there is a developing ice layer. Clearly, if the tube is sufficiently long, the water superheat sufficiently low and/or the vigour of the convective cooling sufficiently great, then the importance of the developing region is reduced accordingly. It is the resulting fully-developed situation which is of principal interest in this paper.

In the spirit of earlier work [1, 2] the analysis is based on the assumption that the latent heat dominates the sensible heat, though without the latter being zero. As will become apparent, the analysis is not limited by this restriction but the icing situation to which it ordinarily applies will be central in the discussion. Consideration will be given to the non-uniformity in the heat transfer coefficient characteristic of a transverse flow. The extent of this non-uniformity, as dictated by the external Reynolds number, will be shown to have an influence on the shape of the ice–water interface and the pressure gradient in the water.

ICE-GROWTH ANALYSIS

Consider heat conduction in the ice produced by sudden and maintained immersion of a circular tube in a coolant (see Fig. 1). Since the tube is taken to be infinitely long the process is governed by the following differential equation:

$$\frac{\partial^2 T}{\partial R^2} + \frac{1}{R}\frac{\partial T}{\partial R} + \frac{1}{R^2}\frac{\partial^2 T}{\partial \Theta^2} = \frac{1}{\kappa_i}\frac{\partial T}{\partial t}. \quad (1)$$

Upon introduction of the normalized variables

$$r = \frac{R}{R_1}, \quad \tau = \frac{k_i(T_f - T_c)}{\rho_i L R_1^2}\cdot\frac{Bi_i}{1 + Bi_i}\cdot t$$

$$\theta = \frac{\Theta}{2\pi}, \quad \phi = \frac{T - T_f}{T_f - T_c}$$

equation (1) becomes

$$\frac{\partial^2 \phi}{\partial r^2} + \frac{1}{r}\frac{\partial \phi}{\partial r} + \frac{1}{4\pi^2 r^2}\frac{\partial^2 \phi}{\partial \theta^2} = \alpha\frac{\partial \phi}{\partial \tau} \quad (2)$$

where $\alpha = Ste_i Bi_i/(1 + Bi_i)$. This simplifies immediately by virtue of the fact that $4\pi^2 \gg 1$, and therefore provided that r is not too close to zero (i.e. the ice is "thin") it follows that

$$\frac{\partial^2 \phi}{\partial r^2} + \frac{1}{r}\frac{\partial \phi}{\partial r} = \alpha\frac{\partial \phi}{\partial \tau} \quad (3)$$

is a good approximation. The solution of equation (3) is subject to the conditions

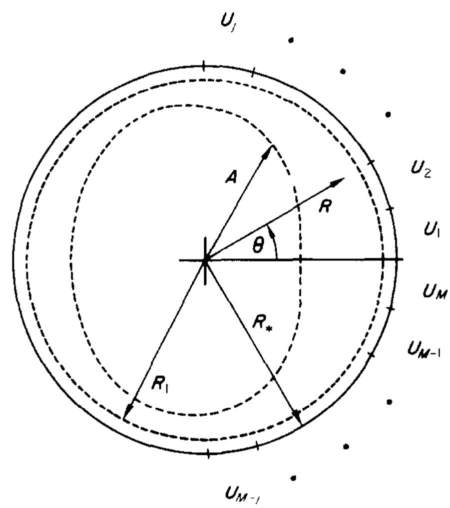

FIG. 1. Co-ordinate system.

$$\phi(r, 0, \alpha) = 0$$

$$\phi(a, \tau, \alpha) = 0$$

$$\frac{\partial \phi}{\partial r}(1, \tau, \alpha) = -Bi_i[1 + \phi(1, \tau, \alpha)].$$

Interface motion is described by a heat balance: thus

$$\rho_i L\frac{\mathrm{d}A}{\mathrm{d}t} = k_i\left(\frac{\partial T}{\partial R}\right)_A$$

or

$$\frac{da}{d\tau} = \frac{1 + Bi_i}{Bi_i} \frac{\partial \phi}{\partial r}(a, \tau, \alpha), \tag{4}$$

the solution of which must satisfy the condition $a(0, \alpha) = 1$ if the system is initially ice free.

In a great many situations the latent heat dominates the sensible heat and hence $Ste_i \ll 1$. Under such circumstances it is clear that α is equally small, or smaller, and this suggests a solution of equation (3) in the form

$$\phi(r, \tau, \alpha) = \phi_0(r, \tau) + \sum_{n=1}^{\infty} \alpha^n \phi_n(r, \tau). \tag{5}$$

Likewise, a solution to equation (4) may be sought in the same form: that is

$$a(\tau, \alpha) = a_0(\tau) + \sum_{n=1}^{\infty} \alpha^n a_n(\tau). \tag{6}$$

Substituting equation (5) into equation (3) generates an infinite set of differential equations for the temperature. The first two of these are:

$$\left.\begin{aligned} &\frac{\partial^2 \phi_0}{\partial r^2} + \frac{1}{r}\frac{\partial \phi_0}{\partial r} = 0 \\ &\frac{\partial^2 \phi_1}{\partial r^2} + \frac{1}{r}\frac{\partial \phi_1}{\partial r} = \frac{\partial \phi_0}{\partial \tau} \end{aligned}\right\} \tag{7}$$

which are to be satisfied subject to the conditions

$$\left.\begin{aligned} &\phi_0(r, 0) = 0 \\ &\phi_0(a_0, \tau) = 0 \\ &\frac{\partial \phi_0}{\partial r}(1, \tau) = -Bi_i[1 + \phi_0(1, \tau)] \\ &\phi_1(r, 0) = 0 \\ &\phi_1(a_0, \tau) = -a_1 \frac{\partial \phi_0}{\partial r}(a_0, \tau) \\ &\frac{\partial \phi_1}{\partial r}(1, \tau) = -Bi_i\, \phi_1(1, \tau). \end{aligned}\right\} \tag{8}$$

Solutions of equations (7) which meet the above requirements are:

$$\phi_0(r, \tau) = -F_0(\tau) \ln \frac{r}{a_0} \tag{9}$$

$$\phi_1(r, \tau) = F_1(\tau)\left[r^2 \ln \frac{r}{a_0} - r^2\left(\frac{F_0 + 1}{F_0}\right)\right] + F_2(\tau) \ln r + F_3(\tau) \tag{10}$$

where

$$F_0(\tau) = \frac{Bi_i}{1 - Bi_i \ln a_0},$$

$$F_1(\tau) = -\frac{da_0}{d\tau}\frac{F_0^2 a_0}{4},$$

$$F_2(\tau) = \frac{F_1}{a_0^2}\left[1 + \frac{2}{Bi_i}\left(1 + \frac{1}{Bi_i}\right)\right] - F_1(1 + F_0) - \frac{F_0^2 a_1}{a_0};$$

and

$$F_3(\tau) = -\frac{F_2}{Bi_i} + \frac{F_1}{a_0^2}\left[1 + \frac{2}{Bi_i}\left(1 + \frac{1}{Bi_i}\right)\right].$$

The solutions (9) and (10) are incomplete because they contain a_0 and a_1 which are unavailable *a priori*. However, these contributions to the interface location may be found by substitution of equations (5) and (6) into equation (4): whence

$$\left.\begin{aligned} &\frac{da_0}{d\tau} = \frac{1 + Bi_i}{Bi_i}\frac{\partial \phi_0}{\partial r}(a_0, \tau) \\ &\frac{da_1}{d\tau} = \frac{1 + Bi_i}{Bi_i}\left[\frac{\partial \phi_1}{\partial r}(a_0, \tau) + a_1 \frac{\partial^2 \phi_0}{\partial r^2}(a_0, \tau)\right]. \end{aligned}\right\} \tag{11}$$

The associated initial conditions are:

$$\left.\begin{aligned} &a_0(0) = 1 \\ &a_1(0) = 0. \end{aligned}\right\} \tag{12}$$

Using equation (9) with the first of equations (11) gives

$$\frac{da_0}{d\tau} = -\frac{1 + Bi_i}{Bi_i} \cdot \frac{F_0}{a_0} \tag{13}$$

which integrates immediately to give

$$\tau = \frac{Bi_i}{1+Bi_i}\left\{\frac{a_0{}^2 \ln a_0}{2} + (1-a_0{}^2)\frac{Bi_i+2}{4Bi_i}\right\}. \quad (14)$$

Now using equations (9), (10) and (13), the second of equations (11) may be written in the form

$$\frac{da_1}{da_0} + \left(\frac{1-F_0}{a_0}\right)a_1 = \frac{1+Bi_i}{Bi_i} \times \left\{\frac{F_0}{2} + \frac{F_0{}^2}{4} + \frac{F_0{}^3}{4} - \frac{F_0{}^3}{4a_0{}^2} \times \left[1 + \frac{2}{Bi_i}\left(1 + \frac{1}{Bi_i}\right)\right]\right\}$$

which integrates readily to give

$$a_1 = \frac{1+Bi_i}{Bi_i}\frac{F_0}{a_0}\left[\frac{a_0^2-1}{4} - \frac{F_0 - Bi_i}{2Bi_i}\left(1 + \frac{1}{Bi^i}\right)\right]. \quad (15)$$

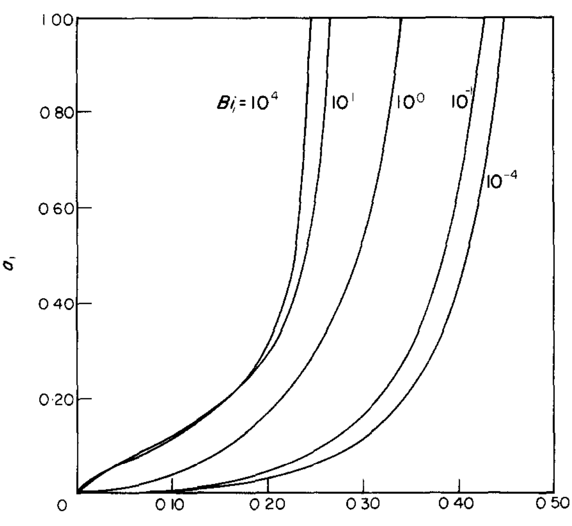

FIG. 2. First-order interface correction.

Since equations (14) and (15) give τ and a_1 as functions of a_0 it follows that both a_1 and a_0 can be expressed as functions of τ. Figure 2 reveals the time-dependency of a_1 for various Biot numbers and Fig. 3 shows the effect of Stefan number and Biot number on interface growth.

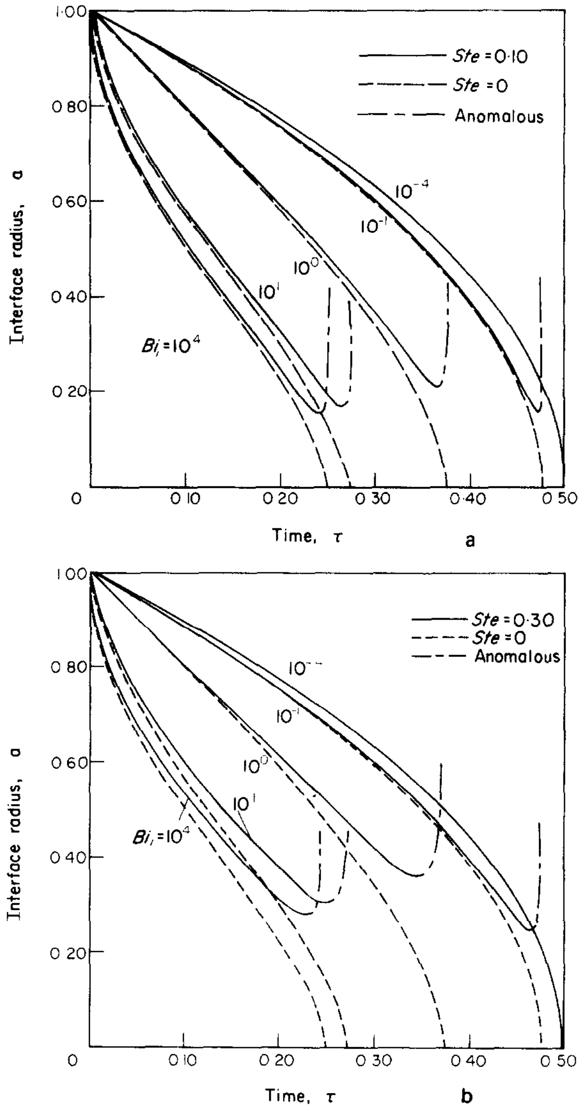

FIG. 3. The effect of sensible heat and convection on ice growth.
(a) $Ste = 0{\cdot}10$.
(b) $Ste = 0{\cdot}30$.

PRESSURE DROP ANALYSIS

Under conditions which produce a close approximation to an axi-symmetric system, the results of the previous section may be used to predict the shape of the ice–water interface generated by circumferential variations in heat transfer coefficient i.e. in the Biot number. This is accomplished using established data for transverse flow over an isothermal cylinder at various values of the external Reynolds number [14]. Figure 4 shows progressive changes in the size and shape of the interface for two selected Reynolds numbers.

and

$$\frac{\partial p}{\partial x} = \frac{\partial P}{\partial X} \bigg/ \left(\frac{\partial P}{\partial X}\right)_{ni}.$$

It is clear from Fig. 4 that the interface does not generally possess a regular shape and therefore it is necessary to use a technique capable of solving equation (16) within arbitrarily-shaped

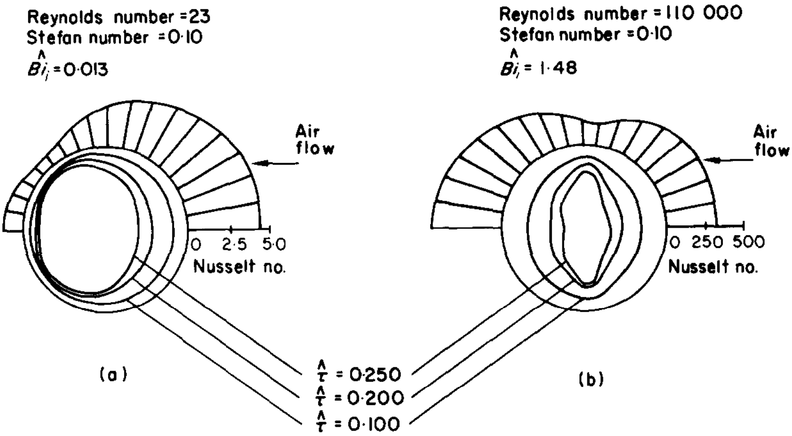

FIG. 4. Ice growth in a transverse air flow.

During growth of the ice shell any water flowing in the tube experiences an increasing resistance attributable to a continual decrease in the area through which it must pass. This poses the question of how the interface growth changes the pressure drop. Knowing the interface shape at any time it now remains to calculate the corresponding pressure gradient as described by the equation†

$$\frac{4\partial p}{\partial x} = \frac{\partial^2 u}{\partial r_*^2} + \frac{1}{r_*}\frac{\partial u}{\partial r_*} + \frac{1}{4\pi^2 r_*^2}\frac{\partial^2 u}{\partial \theta^2} \qquad (16)$$

where

$$u = U \bigg/ \frac{R_*^2}{4\mu}\left(\frac{\partial P}{\partial X}\right)_{ni}$$

$$r_* = R/R_*$$

† Neglect of aximuthal variations is not acceptable in the water because it flows in the vicinity of $r = 0$. Velocity transients are negligible in water if $\alpha \ll 1$.

surfaces. Of several available techniques which might be applied [15–17] that of Sparrow and Haji-Sheikh appears to be the most general: it is semi-analytic, i.e. analytic in formulation but numerical in execution. None of these techniques will be used here and instead it is proposed to develop an alternative semi-analytic method, similar to that employed by Boley [18], which has the merit of relative simplicity. This method treats the region of interest as an interior part of a larger fictitious region of any convenient size and shape. The solution to equation (16) is then readily found for the larger region and adjusted, through the outer boundary values, until values at the surface of the inner region satisfy the boundary conditions of the problem originally specified. The (larger region) solution so obtained then contains the (inner region) solution to the original problem.

Consider the solution of equation (16) in the imbedded region defined by the inner broken curve shown in Fig. 1. This region represents the area available for the flow of water and is an interior part of the larger region bounded by the circle radius R_*. As indicated, the circular outer boundary is divided into a number of segments, taken equal for convenience. Each of these segmental arcs is assumed to have a velocity u_j, the magnitude and sign of which has to be determined. The velocity distribution resulting solely from the motion of any given arc is readily found and by superposition it is clear that for m equally-wide segments the velocity field is given by

$$u(r_*, \theta) = -\frac{\partial p}{\partial x}(1 - r_*^2) - \sum_{j=1}^{m} u_j f_j(r_*, \theta) \quad (17)$$

where

$$f_j(r_*, \theta) = \frac{1}{m} + 2\sum_{n=1}^{\infty} \frac{r_*^n \sin(\pi n/m)}{\pi n} \cos n \left[2\pi\theta - (j - \tfrac{1}{2})\frac{2\pi}{m}\right].$$

This solution is valid within the interior region and represents the solution of the original physical problem if, and only if, the velocity around the ice–water interface is zero. This condition is satisfied when

$$\sum_{j=1}^{m} u_j f_j(a_{*k}, \theta_k) = -\frac{\partial p}{\partial x}(1 - a_{*k}{}^2) \quad (18)$$

where $a_* = A/R_*$, and (a_{*k}, θ_k) are any of m appropriate interface coordinate pairs. It is evident that equations (18) form of a set of m linear algebraic equations relating the adjustable arc velocities u_j to any given set of interface radii a_{*k}, or a_k. Thus for any interface size and shape a′representative set of a_k may be chosen and used to determine the set of u_j which will produce a solution to equation (16) with a no-slip contour passing through the chosen a_k.

As written, equation (18) cannot be solved unless the pressure gradient is specified. To circumvent this difficulty equation (17) is re-written as

$$u(r_*, \theta) = -\frac{\partial p}{\partial x} G(r_*, \theta)$$

thus permitting the calculation of $u_j/(\partial p/\partial x)$ instead of u_j in equation (18). The variation of $\partial p/\partial x$ may now be found from the volumetric flow rate given by

$$\dot{Q} = \int U \, dS$$

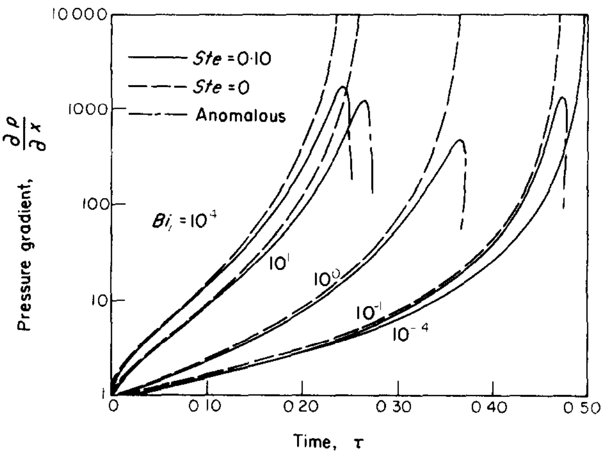

FIG. 5. The effect of sensible heat and convection on pressure gradient.

$$= -\frac{R_*^2}{4\pi}\left(\frac{\partial P}{\partial X}\right)\int G(r_*, \theta)\,\mathrm{d}S.$$

For a constant flow rate this may be equated to the ice-free value,

$$\dot{Q}_{ni} = -\frac{R_1^4}{4\mu}\left(\frac{\partial P}{\partial X}\right)_{ni}\cdot\frac{\pi}{2}.$$

Hence

$$\frac{\partial p}{\partial x} = \frac{\pi}{2}\left(\frac{R_1}{R_*}\right)^4 \Big/ \int G(r_*, \theta)\,\mathrm{d}S_*.$$

The tacit assumption in the above analysis is that R_* is fixed at a value great enough to ensure convergence of $f_j(r_*, \theta)$ but small enough to permit the motion of the arcs around the fictitious boundary to exert sufficient influence at the actual boundary. In dealing with the changing size and shape of the ice–water interface it was considered worthwhile re-establishing R_* for each value of τ at which the pressure drop was determined.

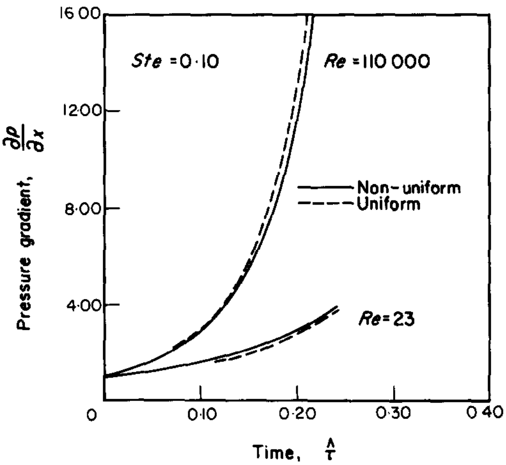

FIG. 6. Pressure steepening in a transverse air flow.

Figure 5 reveals the steepening of the pressure field for various representative values of the Stefan and Biot numbers under uniform external convection. Figure 6 shows similar curves for each of two transverse flows incorporating non-uniform convection under the same conditions considered earlier.

DISCUSSIONS AND CONCLUSIONS

The analysis assumes that the water is not superheated which implies that the pipe is sufficiently long to allow the withdrawal of any inlet superheat, or that the inlet temperature is the freezing temperature. In addition, viscous dissipation has been neglected, thus implying that

$$U_{av} \lesssim 100(Ste_i\, Bi_i)^{\frac{1}{2}} \text{ m/s}.$$

It is clear from this that dissipation will not be important unless Ste_i Bi_i (and hence α) is very small and/or the water velocity is extremely high. For a fixed flow rate, the latter condition undoubtedly occurs when the ice–water interface approaches the axis of the tube and because of this the results are inaccurate when the water occupies only a small region close to the axis.

The effect of ice sensible heat and external convection on ice growth under uniform conditions is shown in Fig. 3. The limiting case of zero Stefan number is essentially that treated by London and Seban [3] and in effect contains the full range of permissible Biot numbers: it should be noted that τ contains Bi_i and therefore differs for each Biot number. The effect of the sensible heat in the ice is revealed by comparing these results with others for which $Ste_i \neq 0$. Since the results are generally accurate to α^2 a somewhat arbitrary upper limit of Ste_i = 0·3 ensures that, regardless of the Biot number, inaccuracies of order 10 per cent will not be exceeded and Fig. 3(b) shows these results. It is immediately evident that sensible heat of this magnitude does not greatly alter the rate of ice growth and that the greatest effect is felt at high Biot numbers, as one might expect. The minima revealed are difficult to explain on physical grounds and results beyond these points are considered unreliable: this type of behaviour stems from truncation of the perturbation expansion. Such a limitation is, however, quite small because the values of τ or a at which first order accuracy is unacceptable are generally beyond the scope of the analysis for other reasons; namely, the neglect of viscous dissipation and circumferential conduction.

It is worth noting that a Stefan number of 0·3 corresponds to a temperature of −48°C which, although it lies within the meteorological realm, is a value below which the atmospheric temperature does not remain too long.† Obviously, higher Stefan numbers would imply an even greater sensible-heat effect but the analysis cannot be used to accurately predict this unless $\alpha \ll 1$. Since the perturbation expansion is in α it becomes especially accurate as an adiabatic boundary condition is *approached*, i.e. $Bi_i \to 0$. Under this condition the interface equation reduces to the simple form

$$a = (1 - 2\tau)^{\frac{1}{2}}. \tag{19}$$

This asymptote is very close to the result shown in Fig. 3 for $Bi_i = 10^{-4}$. It is worth emphasizing that this expression is independent of Stefan number. As a simple explicit form, equation (19) would be useful in the determination of the interface shape and growth from any empirical or analytic expressions for the Biot number when the latter is much less than unity. It is interesting to note that under uniform convection equation (19) leads to the asymptotic pressure gradient relation

$$\frac{\partial p}{\partial x} = \frac{1}{(1 - 2\tau)^2} \tag{20}$$

though it should be added that viscous dissipation could well play an important role under these limiting conditions.

If the tube is immersed in a transverse flow the convection system does not exhibit uniformity as the heat-transfer coefficient varies circumferentially in a manner which depends upon both the external Reynolds number and the Prandtl number of the coolant. Figure 4 shows representative ice–water interface profiles resulting from an air flow at two very different Reynolds numbers: the convection data are taken from [14]. Figure 4a describes the lower Reynolds number situation in which moderate variations in the local Biot (or Nusselt) number result in significant variations in ice thickness, as the low mean Biot number would suggest. The interface geometry during the time interval considered appears to be perfectly compatible with the assumption of quasi-radial symmetry though the validity of such an assumption generally depends upon the circumferential variations in the heat-transfer coefficient.

Similar results for a much higher Reynolds number are shown in Fig. 4b which reveals that variations in ice thickness are less pronounced at a higher mean Biot number: as $Bi_i \to \infty$ it is clear from Fig. 3 that variations would vanish entirely. In this particular example the greatest heat-transfer coefficient occurs at the trailing stagnation point and therefore the ice which first appears at the tube axis would approach from the rear. As the figure indicates the radial-symmetry approximation is doubtful as that moment is approached.

One of the principal objections to the presence of ice in a water pipe is the reduced flow area which it leaves. This implies that flow rates will be reduced or pressure gradients increased, or both. For fixed flow rate conditions the ratio of the pressure gradient to its initial value is shown in Fig. 5 for uniform convection. Again the effect of sensible heat is seen to be rather less than that of external convection.

Figure 6 displays the effect of non-uniform convection for the same conditions described in Fig. 4. It is immediately evident from Fig. 6 that for the time interval considered there is little difference between the pressure gradient for non-uniform convection and the corresponding gradient assuming an average (constant) Biot number. This suggests that the pressure drop could be calculated quite accurately using the hydraulic mean diameter of the interface. Since the latter will not likely possess sharp

† Exceptions to this may be found in many polar and sub-polar regions.

corners it is apparent that the same conclusion would apply to a turbulent flow.

In summary, it might be mentioned that the analysis is valid for any external coolant, the air results shown in Fig. 4 serving merely as examples. Similarly, the treatment is by no means restricted to ice and water though such a system is of great interest. The entire paper is a discussion of the fully-developed situation which may be regarded as the asymptote of the entry-region problem: the latter may possess a steady-state limit without freeze-over but in the absence of viscous dissipation the fully-developed problem is essentially a transient situation in which all the water is eventually frozen. The time scale chosen for this transient problem facilitates the discussion of the limiting cases of infinite heat-transfer coefficient and zero heat-transfer coefficient together with every situation in between.

ACKNOWLEDGEMENT

This work is part of a research programme on ice formation sponsored by the National Research Council of Canada, to whom the authors are indebted.

REFERENCES

1. C. L. Pekeris and L. B. Slichter, Problems of ice formation *J. Appl. Phys.* **10**, 135–137 (1939).
2. J. Stefan, Über die Theorie der Eisbildung insbesondere über die Eisbildung im Polarmeere, *Ann. Phys. u Chem., Neue Folge* **42** (Ht 2), 269–286 (1897).
3. A. L. London and R. A. Seban, Rate of ice formation, *Trans. Am. Soc. Mech. Engrs* **65**, 771–778 (1943).
4. F. Kreith and F. Romie, A study of the thermal diffusion equation with boundary conditions corresponding to solidification or melting of materials initially at the fusion temperature, *Phys. Soc. Proc.* **68B**, Pt 5, 277–291 (1955).
5. D. N. de G. Allen and R. T. Severn, The application of relaxation methods to the solution of non-elliptic partial differential equations. III. Heat conduction, with change of state in two space dimensions, *Q.J. Mech. Appl. Math* **15**, 53–62 (1962).
6. L. C. Tao, Generalized numerical solutions of freezing a saturated liquid in cylinders and spheres, *A.I.Ch.E. Jl* **13**, 165–169 (1967).
7. G. Poots, On the application of integral-methods to the solution of problems involving the solidification of liquids initially at fusion temperature, *Int. J. Heat Mass Transfer* **5**, 525–531 (1962).
8. K. Stephan, Influence of heat transfer on melting and solidification in forced flow, *Int. J. Heat Mass Transfer* **12**, 199–214 (1969).
9. D. C. Baxter, The fusion times of slabs and cylinders, *Trans. Am. Soc. Mech. Engrs, J. Heat Transfer* **84**, 317–326 (1962).
10. R. Siegel and J. M. Savino, Transient solidification of a flowing liquid on a cooled plate including heat capacities of frozen layer and plate, NASA TN D-4353 (1968).
11. R. D. Zerkle and J. E. Sunderland, The effect of liquid solidification in a tube upon laminar-flow heat transfer and pressure drop, *J. Heat Transfer* **90**, 183–190 (1968).
12. M. N. Özisik and J. C. Mulligan, Transient freezing of liquids in forced flow inside circular tubes, *J. Heat Transfer* **91**, 385–390 (1969).
13. G. S. H. Lock, R. D. J. Freeborn and R. H. Nyren, Analysis of ice formation in a convectively cooled pipe, *Proc. 4th Int. Heat Transfer Conf.*, Versailles (1970).
14. J. G. Knudsen and D. L. Katz, *Fluid Dynamics and Heat Transfer*, pp. 497–501. McGraw-Hill, New York (1958).
15. L. N. Tao, Method of conformal mapping in forced convection problems, *Int. Dev. Heat Transfer* 598–606 (1961).
16. K. C. Cheng, Laminar flow and heat transfer characteristics in regular polygonal ducts, *Proc. 3rd Int. Heat Transfer Conf.*, A.I.Ch.E., Chicago, pp. 64–76 (1966).
17. E. M. Sparrow and A. Haji-Sheikh, Flow and heat transfer in ducts of arbitrary shape with arbitrary thermal boundary conditions, *J. Heat Transfer* **88**, 351–358 (1966).
18. B. A. Boley, The analysis of problems of heat conduction and melting, *High Temperature Structures and Materials: Proc. Third Symp. Naval Structural Mechanics*, pp. 260–315. Pergamon Press, London (1963).

ANALYSE DE LA FORMATION PLEINEMENT DÉVELOPPÉE DE GLACE DANS UN TUBE CIRCULAIRE REFROIDI PAR CONVECTION

Résumé—L'article présente une analyse théorique de la formation de glace dans un long tube circulaire, refroidi par convection externe. L'analyse utilise un développement régulier de perturbation pour la température et à l'interface: des solutions de premier ordre sont données sous une forme littérale. On montre, graphiquement, l'effet de la chaleur latente de la glace et la convection externe sur la forme de l'interface et sur le gradient de pression.

ANALYSE DER VOLLAUSGEBILDETEN EISBILDUNG IN EINEM KONVEKTIV GEKÜHLTEN ROHR MIT KREISQUERSCHNITT

Zusammenfassung—Die Arbeit liefert eine theoretische Analyse der Eisbildung in einem langen Rohr mit Kreisquerschnitt, das durch Konvektion von aussen gekühlt wird. Zur Berechnung der Temperaturverteilung und der Lage der Phasengrenze wird die Methode der Störungsrechnung benutzt. Lösungen erster Ordnung werden in geschlossener Form entwickelt. Der Einfluss von fühlbarer Wärme in Eis und äusserer Konvektion auf die Form der Phasengrenze und auf den Druckgradienten wird graphisch gezeigt.

АНАЛИЗ ПОЛНОСТЬЮ РАЗВИТОГО ПРОЦЕССА ОБРАЗОВАНИЯ ЛЬДА В КОНВЕКТИВНО ОХЛАЖДАЕМОЙ ТРУБЕ

Аннотация—В статье проводится теоретический анализ образования льда в длинной круглой трубе, охлаждаемой внешней конвекцией. В анализе используются представление температуры и расположения поверхности раздела фаз в виде регулярных возмущений. Решения первого приближения представлены в замкнутом виде. Приведен график зависимости формы поверхности раздела градиента давления от температуры льда и внешней конвекции.